# Phase and amplitude gradient method for the estimation of acoustic vector quantities

Derek C. Thomas,[a] Benjamin Y. Christensen, and Kent L. Gee
*Department of Physics and Astronomy, Brigham Young University, N283 ESC, Provo Utah 84602*

(Received 29 October 2013; revised 13 January 2015; accepted 19 February 2015)

An alternative pressure-sensor based method for estimating the acoustic intensity, the phase and amplitude gradient estimation (PAGE) method, is presented. This method uses the same hardware as the standard finite-difference method, but does not suffer from the frequency-dependent bias inherent to the finite-difference method. A detailed derivation of the PAGE method and the finite-difference method is presented. Both methods are then compared using simple acoustic fields. The ability to unwrap the phase component of the PAGE method is discussed, which leads to accurate intensity estimates above previous frequency limits. The uncertainties associated with both methods of estimation are presented. It is shown that the PAGE method provides more accurate intensity estimates over a larger frequency bandwidth. © *2015 Acoustical Society of America*.
[http://dx.doi.org/10.1121/1.4914996]

[DKW] Pages: 3366–3376

## I. INTRODUCTION

The method for in-air acoustic intensity measurements using matched microphone sets has been sufficiently refined so that it is the subject of several standards.[1,2] Additional standards have been developed for various applications of intensity measurements, including *in situ* emission pressure level measurements,[3] sound power measurements,[4,5] and determination of sound insulation properties in building acoustics.[6–8] The principles and applications of acoustic intensity are described in a textbook by Fahy[9] and in other handbooks, such as Refs. 10–12. These standards and books deal almost exclusively with a method for estimating acoustic intensity that is commonly referred to as the FD method. This method uses multiple matched microphones to estimate the pressure gradient across the microphones, which corresponds to the particle velocity and thereby the acoustic intensity. This method suffers from a frequency-dependent bias: the method underestimates the intensity as frequency approaches the spatial Nyquist frequency, where half the wavelength of the incoming waves equals the separation distance between microphones within the probe.[13] For the convenience of this work, the finite-difference p-p method is referred to simply as the FD method.

In addition to the FD or p-p method, there are intensity probes based directly on simultaneous pressure and particle velocity measurements, i.e., the p-u method. A commercially available probe uses a pair of heated wires to measure acoustic velocity directly.[14] In environments where significant non-acoustic temperature and velocity fluctuations occur, use of the p-p method has been shown to be more robust.[11,15] Recent efforts to develop and use p-p based probes in the near field of rocket and military jet aircraft plumes[16–19] have served as motivation to examine errors associated with the FD method.

Various studies have investigated how to quantify and reduce errors related to FD processing of p-p probes. These include low-frequency phase mismatch,[20] high-frequency probe performance,[21] and the effect of scattering bias,[22,23] as well as the design of multidimensional probes.[24–27] In recent papers, Wiederhold *et al.*[28,29] reviewed many probe designs and considered different schemes for optimal estimation of sound intensity using the FD method. The foundation for all of these studies is the original FD method, which involves sums and differences of complex pressures or cross spectra.

In this work, we propose a new approach for the calculation of acoustic intensity from measured fields, inspired by the work of Mann *et al.*[30] and Mann and Tichy.[31,32] In these works, it is demonstrated that the active and reactive intensities can be written as

$$\mathbf{I}_a = \frac{1}{\omega\rho_0} P^2 \nabla\phi, \tag{1a}$$

$$\mathbf{I}_r = -\frac{1}{\omega\rho_0} P \nabla P. \tag{1b}$$

These equations are used to investigate the physical meaning of energy-related quantities. When Mann *et al.* compared theoretical results to measured intensities, intensity relations derived from Eqs. (1a) and (1b) were not used in measurement, but instead the traditional FD method was used.[32] We propose that the expressions given by Mann *et al.* can be used to create a new method of estimating acoustic intensity. The expressions, Eqs. (1a) and (1b), were proposed primarily as theoretical tools, whereas the focus of this work will be the application of these expressions to estimate intensity from physical measurements.

The FD method uses a gradient of the complex pressure to determine acoustic intensity. Rather than estimating the pressure gradient from the complex pressures, the gradients

[a]Author to whom correspondence should be addressed. Electronic mail: dcthomas@utexas.edu

of the pressure phase and amplitude can be estimated separately. Using these gradients, along with a center pressure amplitude, the relations in Eqs. (1a) and (1b) can be used to estimate the acoustic intensity. We refer to this method as the phase and amplitude gradient estimation method, or the PAGE method.

This paper develops the mathematical theory of the PAGE method and demonstrates the advantages of this method over the standard FD method. The derivation of the estimation techniques required for both the FD and PAGE methods is given. One primary advantage of the PAGE method over the FD method is that the measured phase differences can be unwrapped, which allows for accurate intensity estimates to be made beyond the spatial Nyquist limit of a probe. A discussion of ensemble averaging of data to obtain intensity estimates is also included, as it differs slightly between the two methods. We then compare the two methods through estimation error of various fields, using two simple probe configurations. It is shown that the PAGE method does not suffer from the frequency-dependent bias and provides better estimates of the intensity. Last, the effects of calibration errors on measurements are considered using an uncertainty analysis.

## II. THEORY

All the derivations in this paper are conducted in the frequency domain; that is, all pressures and particle velocities are assumed to be obtained from the Fourier transform of an appropriate function. Variables with numeric subscripts correspond to those evaluated at position vectors with the same index. For example, $p_1$ is equivalent to $p(\mathbf{r}_1)$, where $\mathbf{r}_1$ is a position vector. The methods presented here assume that the measured field is statistically stationary and ergodic, meaning the statistical properties can be determined with a sufficiently long sample.[22] This assumption allows the development of concise frequency-dependent expressions for the complex intensity in terms of active, $\mathbf{I}_a$, and reactive, $\mathbf{I}_r$, components.

Because both the standard FD method and the new PAGE method for estimating the acoustic intensity can be formulated in terms of least-squares estimates, we first present the formulation of this least-squares estimate. The formulation given here provides the same expressions for the estimated pressure gradient as the method of Pascal and Li.[33] However, the approach developed here is better suited to estimation of the gradient of other field quantities required for this work.

### A. Least-squares estimate of the gradient of a scalar function

A probe consisting of $N$ sensors placed at $N$ unique points with position vectors $\mathbf{r}_1, \mathbf{r}_2, \ldots, \mathbf{r}_N$ can be used to estimate the gradient of a scalar function, $g(\mathbf{r})$. It should be noted the methods presented here require at least one more sensor than the number of dimensions in the system that is to be measured (i.e., two sensors for one-dimensional fields, three sensors for two-dimensional fields, etc.). The estimate is developed in a geometry-independent form by defining the $N(N-1)/2 \times 3$ matrix $\mathbf{X}$ with unique pairwise separation vectors as rows

$$\mathbf{X} = [\mathbf{r}_2 - \mathbf{r}_1 | \mathbf{r}_3 - \mathbf{r}_1 | \cdots | \mathbf{r}_N - \mathbf{r}_{N-1}]^T \tag{2}$$

and the $1 \times N(N-1)/2$ vector of unique pairwise differences of the values of the function $g$ at the sensor positions

$$\boldsymbol{\delta}(g) = \begin{bmatrix} g(\mathbf{r}_2) - g(\mathbf{r}_1) \\ g(\mathbf{r}_3) - g(\mathbf{r}_1) \\ \vdots \\ g(\mathbf{r}_N) - g(\mathbf{r}_{N-1}) \end{bmatrix}. \tag{3}$$

The gradient of $g(\mathbf{r})$ can be estimated using this expression obtained from a multivariate Taylor series

$$\mathbf{X}\nabla g = \boldsymbol{\delta}(g) + O\{\max[\mathbf{X}\nabla(\nabla g)\mathbf{X}^T]\}, \tag{4}$$

where $\nabla(\nabla g)$ is the matrix of second-order derivatives of the function $g$ (the Hessian matrix). The order of the error in Eq. (4) is approximately proportional to the product of the maximum second derivative and the square of the maximum separation distance between sensors. Because the Hessian matrix can be related to the curvature of isosurfaces in the field, $g$, Eq. (4) implies that the local maximum "radius of curvature" of the field $g$ must be large relative to the square of the maximum separation distance of the sensors in the probe. In other words, the field must be close to planar in the neighborhood of the probe.

For probe configurations in which the product of the squared maximum separation distance with the maximum second derivative is sufficiently small compared to the function value, a first-order estimate is obtained from the least-squares solution for the over-determined system in Eq. (4):

$$\widehat{\nabla g} = (\mathbf{X}^T\mathbf{X})^{-1}\mathbf{X}^T\boldsymbol{\delta}(g). \tag{5}$$

The overhat is used to indicate estimated quantities. The matrix inversion in Eq. (5) requires that $\det(\mathbf{X}^T\mathbf{X}) \neq 0$. A necessary and sufficient condition to be able to invert the matrix $\mathbf{X}^T\mathbf{X}$ for a two-dimensional probe is that the sensors not lie on a line; for a three-dimensional probe, the sensors cannot lie in a plane.

### B. FD method

The FD method relies on a least-squares estimate of the gradient of the complex pressure. The FD estimate of the gradient of a pressure field, $p$, is given by Eq. (5) as

$$\widehat{\nabla p} = (\mathbf{X}^T\mathbf{X})^{-1}\mathbf{X}^T\boldsymbol{\delta}(p). \tag{6}$$

The expression for the estimated pressure gradient, $\widehat{\nabla p}$, in Eq. (6) is a linear combination of the pressures measured at the sensor locations. This estimated pressure gradient may then be used to estimate the acoustic intensity in the frequency domain as

$$\widehat{\mathbf{I}}_c = \frac{j}{\rho_0\omega} p_0 \widehat{\nabla p}^*, \tag{7}$$

where $p_0 = p(\mathbf{r}_0)$, where $\mathbf{r}_0$ is the "center of mass" of the probe

$$\mathbf{r}_0 = \frac{1}{N}\sum_{i=1}^{N}\mathbf{r}_i. \tag{8}$$

The work of Wiederhold *et al.*[28,29,34] gives a detailed analysis of optimal methods of finding $p_0$ given different probe configurations. In these works, Wiederhold *et al.* discuss different finite-sum and -difference processing methods and their associated biases. Unless a microphone exists at the center of a probe configuration, the work of Wiederhold *et al.* must be considered to attain optimal intensity estimates for a given probe configuration. If a microphone exists at the center of the probe, such as in the probe used by Miah *et al.*,[35] $p_0$ is the complex pressure measured by the center microphone.

### C. PAGE method

The new PAGE method uses estimates of the phase gradient and amplitude gradient of a pressure field to estimate the acoustic intensity. The PAGE method is most easily developed using the notation of Mann and Tichy.[30] First, the complex pressure is separated into amplitude and phase components

$$p(\mathbf{r}) = P(\mathbf{r})e^{-j\phi(\mathbf{r})}, \tag{9}$$

where $P$ and $\phi$ are real, scalar functions of the position $\mathbf{r}$, representing the amplitude and phase of the pressure, respectively. The gradient of the pressure, $p$, can be written in terms of $P$ and $\phi$ as

$$\nabla p(\mathbf{r}) = [\nabla P(\mathbf{r}) - jP(\mathbf{r})\nabla\phi(\mathbf{r})]e^{-j\phi(\mathbf{r})}. \tag{10}$$

The active and reactive components of the intensity can be rewritten as

$$\mathbf{I}_a = \frac{1}{\omega\rho_0}P^2\nabla\phi, \tag{11a}$$

$$\mathbf{I}_r = -\frac{1}{\omega\rho_0}P\nabla P. \tag{11b}$$

Our work uses these expressions derived by Mann and Tichy[30] as a starting point. We observe that an estimate of $\mathbf{I}$ can be obtained from estimates of $P$, $\nabla\phi$, and $\nabla P$.

First, using the same least-squares estimate as Eq. (6), $\nabla\phi$ is estimated as

$$\widehat{\nabla\phi} = (\mathbf{X}^T\mathbf{X})^{-1}\mathbf{X}^T\boldsymbol{\delta}(\phi), \tag{12}$$

where $\boldsymbol{\delta}(\phi)$ represents a vector of pairwise phase differences, which must be obtained from the measurements of pressure. The phase difference between two sensors can be found from the transfer function

$$\phi(\mathbf{r}_j) - \phi(\mathbf{r}_i) = \arg\{e^{j(\phi(\mathbf{r}_j)-\phi(\mathbf{r}_i))}\} \tag{13}$$

$$= -\arg\{e^{-j(\phi(\mathbf{r}_j)-\phi(\mathbf{r}_i))}\} \tag{14}$$

$$= -\arg\left\{\frac{p_j}{p_i}\right\} \tag{15}$$

$$= -\arg\{H_{ji}\}. \tag{16}$$

Thus the vector of pairwise phase differences, $\boldsymbol{\delta}(\phi)$, is given by the pairwise transfer functions as follows:

$$\boldsymbol{\delta}(\phi) = -\begin{bmatrix} \arg\{H_{12}\} \\ \arg\{H_{13}\} \\ \vdots \\ \arg\{H_{N-1,N}\} \end{bmatrix}. \tag{17}$$

Because the phase differences can be obtained directly from the transfer functions, it is preferable to estimate $\nabla\phi$ using the method presented in Sec. II A rather than using a least-squares estimate of the total phase, $\phi$, which would require the application of the arg function directly to the pressure measurements $p_i$ to obtain the value of $\phi$ at each sensor location.

Next, the pressure amplitudes are found by taking the magnitudes of the measured complex pressures

$$P_i = |p_i|. \tag{18}$$

The pressure amplitude gradient, $\nabla P$, can be estimated using the same least-squares estimate as the previous gradients

$$\widehat{\nabla P} = (\mathbf{X}^T\mathbf{X})^{-1}\mathbf{X}^T\boldsymbol{\delta}(P), \tag{19}$$

where $\boldsymbol{\delta}(P)$ represents the vector of pairwise differences of the measured pressure amplitudes $(P_i)$,

$$\boldsymbol{\delta}(P) = \begin{bmatrix} P_2 - P_1 \\ P_3 - P_1 \\ \vdots \\ P_N - P_{N-1} \end{bmatrix}. \tag{20}$$

The pressure amplitude at the center of the probe must also be found. If there is a microphone at the center of the probe, $P_0$ is found by taking the magnitude of the complex pressure of the center microphone. If a configuration without a center microphone is used, an analysis similar to the work of Wiederhold *et al.* must be employed.[28,29,34]

Using these estimated quantities, we can now estimate the reactive and active intensities as

$$\widehat{\mathbf{I}}_a = \frac{1}{\omega\rho_0}P_0^2\widehat{\nabla\phi}, \tag{21a}$$

$$\widehat{\mathbf{I}}_r = -\frac{1}{\omega\rho_0}P_0\widehat{\nabla P}. \tag{21b}$$

### D. Phase unwrapping

Multi-microphone intensity probes are generally limited to an upper frequency limit, determined by the separation

distance between microphones. This limit, which we will call the spatial Nyquist limit, occurs when $kd = \pi$, where $k$ is the wavenumber, and $d$ is the separation distance between microphones. The FD method suffers from a frequency-dependent bias, where the intensity magnitude is underestimated as $kd$ approaches $\pi$. Past the spatial Nyquist limit, the direction and the magnitude of the intensity estimates given by the FD method become completely unreliable. While the PAGE method does not suffer from the same inherent frequency-dependent bias as the FD method, it still normally gives incorrect estimates past the spatial Nyquist limit. Given certain measurement source characteristics, this limit can be surpassed by unwrapping the phase differences in the argument of the transfer functions.

The phase differences used in the PAGE method are found by taking the argument of the transfer functions between microphones, $\arg\{H_{ij}\}$. The argument function is limited between $-\pi$ and $\pi$, and as such, when the phase function between two microphones is greater than $\pm\pi$ the phase function will wrap. For example, a phase difference of $1.1\pi$ will wrap to $-0.9\pi$. The phase difference between microphones will equal $\pm\pi$ when half the acoustic wavelength is equal to the separation distance between the microphones, also known as the spatial Nyquist limit. These wrapped phase differences result in incorrect phase gradients and thus provide meaningless intensity estimates. When measuring a broadband response, the phase differences function in the frequency domain will be continuous up to the spatial Nyquist limit. At this point, the phase function will wrap and exhibit a $\pm 2\pi$ jump. If we use a simple "unwrap" function, this discontinuity can be corrected by adding $\pm 2\pi$ to the phase function in frequencies above the discontinuity. Because this type of unwrapping requires a continuous phase function, a broadband source is required. This phase function unwrapping allows for accurate phase gradient components past the spatial Nyquist limit, which in turn allows for accurate intensity estimates well past the spatial Nyquist limit.

With a noise-free measurement, there is no upper frequency limit to the PAGE method if the phase function is unwrapped. In practice, noise in the argument of the transfer function will limit the extent to which the phase function can be unwrapped. A noisy transfer function will cause the argument of the transfer function to have multiple discontinuities when the function approaches the $\pm\pi$ limit. If just one of the occurring $2\pi$ jumps is not correctly accounted for, the entire function past that frequency will be incorrect. Thus, minimizing the noise in the transfer functions allows for a larger range of correctly unwrapped phase differences and thus a larger range of accurate intensity estimates. The primary means of minimizing noise in the transfer function is through ensemble averaging, which is discussed in Sec. II E.

### E. Averaging

When applying either the FD or the PAGE method to physical data, it can be advantageous to apply averaging, especially with non-repeatable noise sources. The averaging required for the FD method is relatively simple: the time waveform is broken into blocks, and then the complete intensity processing as discussed above is applied to each block. Each block will then have an associated intensity vector. The average of these vectors is the complete averaged intensity. This approach will provide the same result as averaging the individual cross-spectra and then computing the intensity estimates.

Because the PAGE method relies on the phase of the transfer function, the order of operations with ensemble averaging must be more carefully considered. To obtain the most accurate time-averaged intensity, the transfer functions, $H_{12}$, $H_{13}$, etc., of each block are calculated. These transfer functions are then averaged, and the averaged transfer functions are used in the PAGE calculations. For example,

$$H_{12,\text{avg}} = \frac{1}{N}\sum_{n=1}^{N} H_{12,n}, \tag{22}$$

where $N$ is the total number of blocks, and $n$ represents the index of each block. The argument of these averaged transfer functions is then used in the PAGE method calculations and result in $\widehat{\nabla\phi}_{\text{avg}}$. Similarly, the pressure amplitudes, $P_{i,\text{avg}}$, can be found by calculating $P_i$ for each block and taking the mean. The averaged pressure amplitudes are then used to calculate $\widehat{\nabla P}_{\text{avg}}$ using the same method outlined earlier. The quantities $P_{i,\text{avg}}$, $\widehat{\nabla P}_{\text{avg}}$, and $\widehat{\nabla\phi}_{\text{avg}}$ are then combined to create a single averaged intensity estimate.

As discussed in Sec. II D, the upper frequency limit of the unwrapped PAGE method will depend on the noise in the argument of the transfer functions between microphones. Ensemble averaging, as discussed here, helps smooth the transfer functions, and helps the phase to be unwrapped at higher frequencies. The trade-off with ensemble averaging is that the spectral resolution decreases as the number of averages increases.

## III. COMPARISON OF FD AND PAGE INTENSITY ESTIMATES

We now compare the accuracy of the intensity estimates produced by the finite-difference method to those produced by the PAGE method. First, we consider a one-dimensional intensity probe with two ideal microphones separated by a distance, $d$, in a plane wave of axial incidence. Given the pressure from a plane wave traveling in the $x$ direction,

$$p(x) = Ae^{-jkx}, \tag{23}$$

where $A$ is the acoustic pressure amplitude and $k$ is the wavenumber, the intensity of the wave is

$$\mathbf{I}(x) = \frac{k|A|^2}{\rho_0\omega}\hat{\mathbf{x}}, \tag{24}$$

where $\omega$ is the angular frequency, $\rho_0$ is the fluid mass density, and $\hat{\mathbf{x}}$ is a unit vector in the $x$ direction. Given two microphones at locations

$$r_1 = -\frac{d}{2}, \quad r_2 = \frac{d}{2}, \tag{25}$$

the literature[11] shows that the FD method estimates the intensity as

$$\hat{\mathbf{I}}_a^{\mathrm{FD}} = -\frac{1}{\omega\rho_0 d}\mathrm{Im}\{S_{12}(\omega)\}\hat{\mathbf{x}}, \tag{26}$$

where $S_{ij}$ represents the cross-spectrum of the two complex pressure measurements. This same result can be obtained using the method given in Sec. II B,

$$\hat{\mathbf{I}}_c^{\mathrm{FD}} = \frac{j}{\omega\rho_0}\left(\frac{p_1+p_2}{2}\right)\left(\frac{p_2-p_1}{d}\right) * \hat{\mathbf{x}} \tag{27}$$

$$= \frac{j}{2\omega\rho_0 d}\left(p_1p_2^* - p_1p_1^* + p_2p_2^* - p_2p_1^*\right)\hat{\mathbf{x}}. \tag{28}$$

Taking the real part of this equation and representing the cross spectrum as $S_{ij}$ gives us

$$\hat{\mathbf{I}}_a^{\mathrm{FD}} = \frac{1}{2\omega\rho_0 d}\mathrm{Re}\{j(S_{12} - |p_1| + |p_2| - S_{21})\}\hat{\mathbf{x}}. \tag{29}$$

This equation simplifies to Eq. (26) since $|p_1| = |p_2|$ for a plane wave. This expression provides an accurate approximation for intensity at low values of $kd$, but underestimates the intensity as $kd$ approaches $\pi$.

Using the results of Sec. II C, the estimate given by the PAGE method is calculated as

$$\hat{\mathbf{I}}^{\mathrm{PAGE}} = \frac{-\arg\{H_{12}\}}{\omega\rho_0 d}\left(\frac{|p_1|+|p_2|}{2}\right)^2\hat{\mathbf{x}}. \tag{30}$$

This equation simplifies to

$$\hat{\mathbf{I}}^{\mathrm{PAGE}} = \frac{-\arg\{H_{12}\}}{\omega\rho_0 d}|A|^2\hat{\mathbf{x}} \tag{31}$$

because $|p_1| = |p_2| = |A|$ for a plane wave. The phase of a plane wave is given by $kx$, so the difference of phases of two microphones, $-\arg(H_{12})$, separated a distance, $d$, will simplify to $kd$, as long as $kd < \pi$, which is the spatial Nyquist limit of the probe. Within this limit, the expression for the intensity simplifies to

$$\hat{\mathbf{I}}^{\mathrm{PAGE}} = \frac{kd}{\omega\rho_0 a}|A|^2 \tag{32}$$

$$= \frac{k|A|^2}{\rho_0\omega} \quad (kd < \pi), \tag{33}$$

which is the exact expression for the intensity of a plane wave given in Eq. (24). Simply put, an intensity probe with two ideal microphones can perfectly estimate intensity in one dimension with the PAGE method as long as $kd < \pi$. Furthermore, if phase unwrapping is applied (Sec. II D), there is no theoretical frequency limit for the one-dimensional PAGE method applied to plane waves. Figure 1 shows the magnitude of the error in estimating the plane wave with both the FD and PAGE methods. It can be seen that the PAGE method significantly outperforms the FD at all but the lowest values of $ka$. The PAGE method produces estimates with no error below the spatial Nyquist limit, and if phase unwrapping is used, the PAGE method would have no error for any value of $ka$.

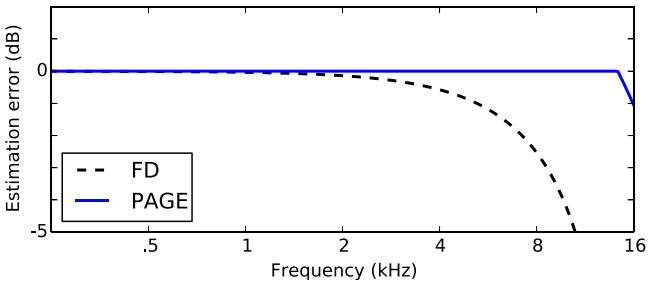


FIG. 1. (Color online) FD and PAGE estimation error given an ideal two-microphone sound intensity probe in a plane wave of axial incidence. The $x$-axis is shown in terms of $kd$, where $k$ is the wavenumber and $d$ is the separation distance between the microphones. Phase unwrapping is not applied to the PAGE estimate.

We now consider intensity estimates in multiple dimensions. This is accomplished by comparing analytically derived intensities of two-dimensional fields to intensity estimates of the same fields given a two-dimensional, four-microphone probe. Two fields are considered: a plane wave and a three-source system. Both pressure fields considered have reflection symmetry, and the probe is confined to the plane of reflection. First, the derivation of the intensity expressions generated by the FD and PAGE methods for a two-dimensional probe is demonstrated.

### A. FD and PAGE expressions for a two-dimensional probe

The chosen probe geometry is an equilateral triangle with a sensor at the center. This is similar to the design evaluated by Suzuki *et al.*,[36] except that the center microphone is lowered so that all the microphones are in the same plane. Each of the outside microphones is placed 2 in. from the center microphone. Using this geometry, $p_0$ and $P_0$ can be determined from the center microphone. It must be noted that without a sensor in the center of the probe, the approach developed by Wiederhold *et al.*[28,29,34] must be employed.

If $a$ is the radius of the circle that circumscribes the probe, then the two-dimensional position vectors of the probe sensors relative to the probe center are

$$\mathbf{r}_1 = \begin{bmatrix}0\\0\end{bmatrix}, \quad \mathbf{r}_2 = a\begin{bmatrix}0\\1\end{bmatrix},$$
$$\mathbf{r}_3 = \frac{a}{2}\begin{bmatrix}\sqrt{3}\\-1\end{bmatrix}, \quad \mathbf{r}_4 = -\frac{a}{2}\begin{bmatrix}\sqrt{3}\\1\end{bmatrix}. \tag{34}$$

Given this probe configuration, the complex intensity as estimated by the FD method is

$$\hat{\mathbf{I}}_c^{\mathrm{FD}} = \frac{-j}{6\rho_0\omega a}\begin{bmatrix}\sqrt{3}(G_{31}-G_{41})\\2G_{21}-G_{31}-G_{41}\end{bmatrix}, \tag{35}$$

where $G_{ij} = 2p_i^*p_j$. The equations to estimate the active and reactive intensity using the PAGE method are

$$\hat{\mathbf{I}}_a^{\mathrm{PAGE}} = -\frac{P_1^2}{6a\omega\rho_0}\begin{bmatrix}\sqrt{3}\arg\{H_{34}\}\\ \arg\{H_{23}\}+\arg\{H_{24}\}\end{bmatrix}, \tag{36}$$

$$\hat{\mathbf{I}}_r^{\mathrm{PAGE}} = -\frac{P_1}{6a\omega\rho_0}\begin{bmatrix}\sqrt{3}(P_3-P_4)\\ 2P_2-P_3-P_4\end{bmatrix}. \tag{37}$$

The derivations of these equation can be found in the Appendix.

We consider the application of the expressions given in Eqs. (35)–(37) to ideal fields. It should be noted that instead of explicitly calculating the estimated intensity in terms of cross-spectra and transfer functions, it can be simpler to leave the derivations in terms of component matrices and vectors. For example, once $P_0$, $\boldsymbol{\delta}(\phi)$, and $\mathbf{X}$ are known, Eq. (36) can be computed in one line as

$$\hat{\mathbf{I}}_a^{\mathrm{PAGE}} = \frac{1}{\omega\rho_0}P_0^2(\mathbf{X}^T\mathbf{X})^{-1}\mathbf{X}^T\boldsymbol{\delta}(\phi). \tag{38}$$

### B. Plane wave

Using the expressions developed previously, we again investigate estimation error of a plane wave. Two quantities are used to evaluate the accuracy of the estimation methods: the error in the amplitude

$$|\mathbf{I}|^{\%\mathrm{err}} = 100\frac{||\hat{\mathbf{I}}|-|\mathbf{I}||}{|\mathbf{I}|}, \tag{39}$$

and the angle between the estimated and exact intensity vectors

$$\theta^{\mathrm{err}} = \arccos\frac{\hat{\mathbf{I}}\cdot\mathbf{I}}{|\hat{\mathbf{I}}||\mathbf{I}|}. \tag{40}$$

The results are presented in Figs. 2 and 3. The error is shown using shades of gray to represent error ranges; all white regions correspond to $<1\%$ error in amplitude (Fig. 2) or $<0.01^\circ$ in error in the estimated direction (Fig. 3). All black regions correspond to amplitude error $>30\%$ or error in the estimated direction $>1^\circ$. The various shades of gray correspond to intermediate ranges.

Figure 2 shows the error in the intensity magnitude estimated with the FD [Fig. 2(a)] and PAGE [Fig. 2(b)] methods, where no phase unwrapping is applied to the PAGE method. It can be seen that both methods break down past the spatial Nyquist point, where the wavelength of the impinging plane wave becomes equal to the largest microphone separation distance parallel to the direction of wave propagation. This occurs near $kd = \pi$, where $d$ is the maximum microphone separation distance. Since the largest sensor separation distance parallel to the impinging wave depends on rotation, this limit varies, as can be seen in Fig. 2(b). If phase unwrapping is used with the PAGE method, it will no longer break down at the spatial Nyquist limit and will result in negligible error over all frequencies. The frequency bias inherent to the FD method is apparent, where the estimation error increases as frequency increases. While this bias is reduced by using the center microphone

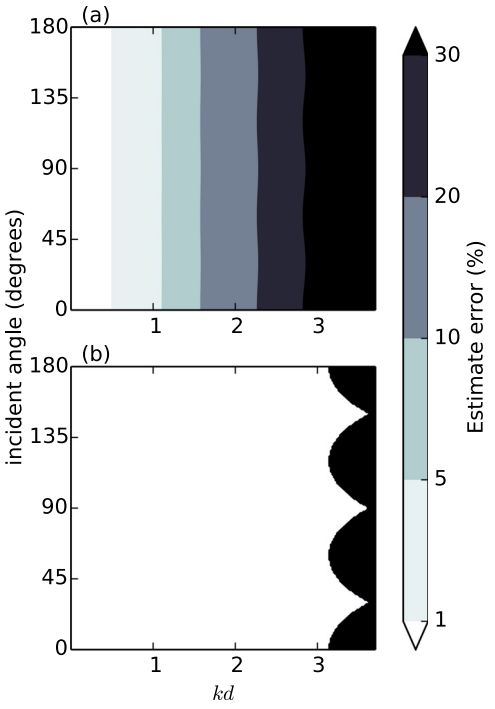


FIG. 2. (Color online) The intensity amplitude estimation error of the (a) FD and (b) PAGE methods as functions of probe rotation angle $\theta$ (measured in degrees) and $kd$, where $k$ is the wavenumber, and $d$ is the maximum microphone separation distance within the probe.

for the pressure component of intensity,[34] it can still be clearly seen in Fig. 2 where the estimation error of the FD method increases as $kd$ increases. The PAGE method does not suffer from this same bias as it gives accurate estimates

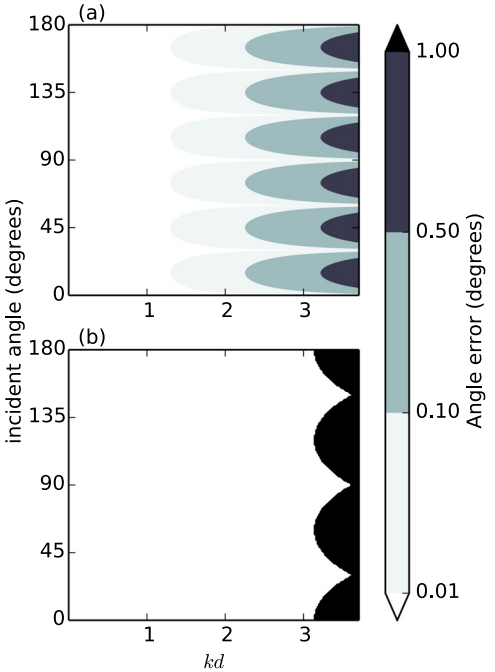


FIG. 3. (Color online) Error in the estimated angle of the acoustic intensity. The error in the angles estimated by the (a) FD and (b) PAGE methods as functions of probe rotation angle $\theta$ (measured in degrees) and $kd$, where $k$ is the wavenumber, and $d$ is the maximum microphone separation distance within the probe.

up to the spatial Nyquist limit of the probe. Thus, we see that for propagating plane wave fields measured by the two-dimensional probe in question, the PAGE method provides better intensity estimates. Though the results are only shown for a particular probe configuration, similar results can be seen with other probe types.

### C. Three-source system

A more complicated acoustic intensity field can be created with three evenly spaced monopoles on a line, with the middle monopole 180° out of phase with the other two. The pressure at any field point is

$$p(\mathbf{r}) = \sum_{i=1}^{3} A_i \frac{e^{-jk|\mathbf{r}-\mathbf{r}_i|}}{|\mathbf{r}-\mathbf{r}_i|}, \tag{41}$$

where $A_1 = 1$ Pa m, $A_2 = -1$ Pa m, $A_3 = 1$ Pa m, and $\mathbf{r}_1 = [-0.18, 0, 0]^{\mathrm{T}}$ m, $\mathbf{r}_2 = [0, 0, 0]^{\mathrm{T}}$ m, $\mathbf{r}_3 = [0.18, 0, 0]^{\mathrm{T}}$ m. The particle velocity is

$$\mathbf{u}(\mathbf{r}) = \sum_{i=1}^{3} -j \frac{A_i}{k\rho_0 c_0} \frac{\mathbf{r}-\mathbf{r}_i}{|\mathbf{r}-\mathbf{r}_i|^3} (1 + jk|\mathbf{r}-\mathbf{r}_i|) e^{-jk|\mathbf{r}-\mathbf{r}_i|}. \tag{42}$$

Figure 4 shows the active acoustic intensity of this field. The expressions for the estimated active intensities given in Eqs. (35) and (36) are used to predict the intensities over the domain shown, and the error of these estimates [given by Eqs. (39) and (40)] is presented in Figs. 5 and 6. By looking at the

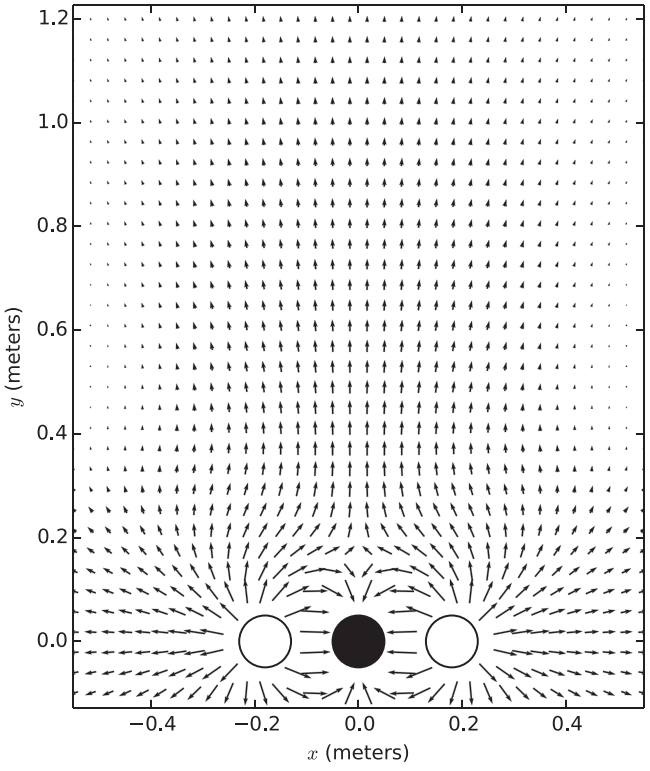


FIG. 4. Active intensity produced by a system of three simple sources spaced evenly on a line, with the center source 180° out of phase with the others. The frequency is 400 Hz, and the sources are spaced 18 cm apart.

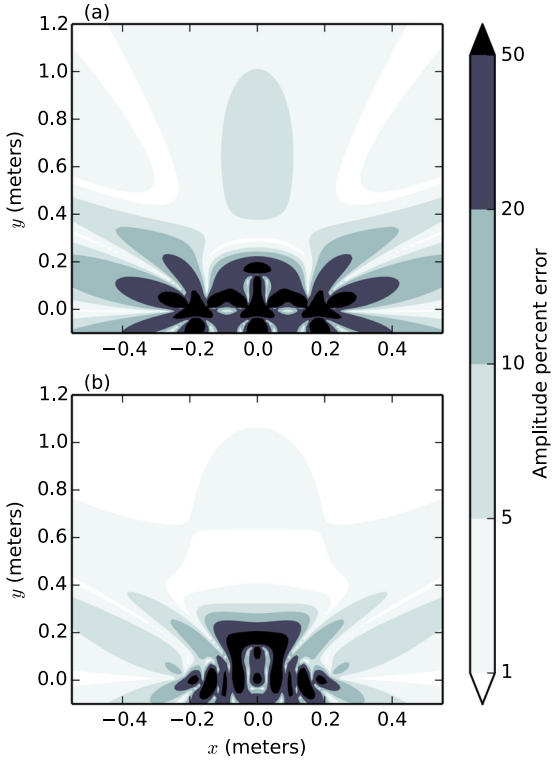


FIG. 5. (Color online) Error in the estimated magnitude of the active intensity at 400 Hz of the three-source system shown in Fig. 4 for the (a) FD and (b) PAGE methods. Estimates are calculated using the two-dimensional probe described in Eq. (A1).

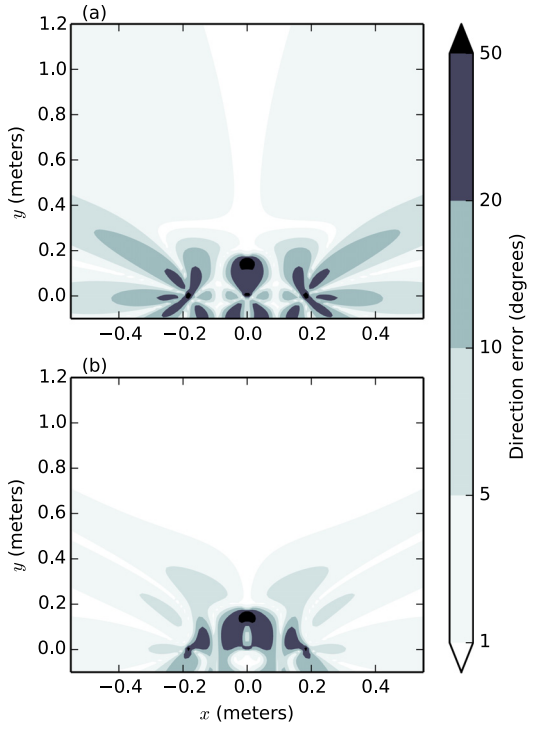


FIG. 6. (Color online) Error in the estimated direction of the active intensity for the three-source system shown in Fig. 4 for the (a) FD and (b) PAGE methods. Estimates are calculated using the two-dimensional probe described in Eq. (A1).

estimation errors of this complicated intensity field, we can determine how both the methods presented perform in complicated fields. In the near field of these monopoles there will be significant reactive components of the intensity, but the evaluation of the PAGE and FD method for reactive intensities is not considered at this time. The probe used to evaluate these fields has a microphone separation distance ($a$) of 5.08 cm (2 in.), which results in a maximum separation distance, $d$, of 8.8 cm. The frequency being evaluated is 400 Hz, which leads to a $kd$ of 0.645. Shades of gray again represent error ranges. The range of errors for this field is greater than in the case of the plane wave and so the error ranges are larger.

The black regions near the sources indicate that both the FD and PAGE methods fail to accurately represent the acoustic intensity in these regions. It is clear that away from the complicated near field of the three monopoles, both methods give reasonable results for the active intensity. However, the PAGE method gives more accurate results than the FD method across most of the near field. These figures only show results at a single frequency, but a similar pattern is seen over all frequencies: the PAGE method consistently outperforms the FD method.

## IV. ERROR ANALYSIS

Both the FD and PAGE methods rely on phase-matched microphones. At low frequencies, even small phase errors between microphones cause large errors in intensity estimates. Phase calibration of microphones can help minimize the errors caused by phase mismatch. In addition, the impact of phase mismatch is lessened when the distance between microphones is increased.

At high frequencies, sound scattering off the body of an intensity probe can cause errors in acoustic intensity. This can be reduced by minimizing the scattering surfaces of the probe and by increasing the separation distance between microphones. However, the spatial Nyquist limit is proportional to the inverse of the separation distance, and so increasing microphone separation reduces the spatial Nyquist limit. This has led to most acoustic intensity probes employing closely spaced microphones, thus sacrificing accuracy at low frequencies for a larger frequency range. As discussed in Sec. II D, the phase components of the PAGE method can be unwrapped, and accurate results can be obtained beyond the spatial Nyquist limit in appropriate fields. The use of phase unwrapping permits larger separation distances to be used without losing the ability to estimate the intensity at higher frequencies. Thus, the problems of both phase mismatch at low frequencies and scattering at high frequencies can be mitigated by increasing the microphone separation. The size of an intensity probe using the PAGE method still needs to remain small enough that the field is locally planar.

### A. Uncertainty analyses

As the PAGE method is new, this section will give a more complete example of how small phase errors affect the accuracy of acoustic intensity estimates produced by the method. For this section, we will be using overbars to denote actual values, so for example, if $p$ is the measured pressure, $\bar{p}$ would be the actual pressure.

First, we will assume that the measurable pressure amplitude and phase are both random variables normally distributed about their physical values, so

$$P \sim \mathcal{N}(\bar{P}, \sigma_P^2) \tag{43}$$

and

$$\phi \sim \mathcal{N}(\bar{\phi}, \sigma_\phi^2). \tag{44}$$

The complex pressure can then be simulated by combining these two random variables

$$p = Pe^{j\phi}. \tag{45}$$

By assuming the different phase and amplitude random variables are independent, the difference between these will also be normally distributed. Thus, we can write the vectors of phase and amplitude differences as

$$\boldsymbol{\delta}(\phi) \sim \mathcal{N}\left(\overline{\boldsymbol{\delta}(\phi)}, \sigma_{\boldsymbol{\delta}(\phi)}^2\right) \tag{46}$$

and

$$\boldsymbol{\delta}(P) \sim \mathcal{N}\left(\overline{\boldsymbol{\delta}(P)}, \sigma_{\boldsymbol{\delta}(P)}^2\right). \tag{47}$$

Furthermore, because of the assumed independence, we know that

$$\sigma_{\boldsymbol{\delta}(\phi)}^2 = 2\sigma_\phi^2 \tag{48}$$

and

$$\sigma_{\boldsymbol{\delta}(P)}^2 = 2\sigma_P^2. \tag{49}$$

Following the work of Szuberla *et al.*,[37] we can now find the variance in the gradient of the phase and amplitude by defining

$$\mathbf{C} = \mathbf{X}^T\mathbf{X}, \tag{50}$$

$$\mathbf{D} = \mathbf{E}^T\mathbf{C}\mathbf{E} = \begin{bmatrix} \lambda_1 & 0 & \cdots & 0 \\ 0 & \lambda_2 & & \\ \vdots & & \ddots & \vdots \\ 0 & & \cdots & \lambda_n. \end{bmatrix}, \tag{51}$$

where $\mathbf{C}$ is the sensor separation covariance matrix, $\mathbf{E}$ is a matrix of eigenvectors of $\mathbf{C}$, and $\mathbf{D}$ is a diagonal matrix of eigenvalues. The variances of the gradients can be written as

$$\sigma_{\nabla\phi,n} = \sqrt{\frac{\sigma_{\boldsymbol{\delta}(\phi)}^2}{\lambda_n}}, \tag{52}$$

$$\sigma_{\nabla P,n} = \sqrt{\frac{\sigma_{\boldsymbol{\delta}(P)}^2}{\lambda_n}}, \tag{53}$$

where $\lambda_n$ represents the eigenvalues in $\mathbf{D}$. The eigenvectors in $\mathbf{E}$ define the rotation of the coordinates from the principal axis. Thus, we can represent the phase and amplitude gradients in terms of multivariate Gaussians, centered at the location of the actual values with covariance defined by $\mathbf{C}$. These can be combined with the Gaussian pressure amplitudes to simulate the intensity as

$$\mathbf{I}_a^{\text{PAGE}} = \frac{1}{\omega\rho_0} P^2 \nabla\phi, \tag{54}$$

$$\mathbf{I}_r^{\text{PAGE}} = -\frac{1}{\omega\rho_0} P \nabla P, \tag{55}$$

where

$$P \sim \mathcal{N}(\bar{P}, \sigma_P^2), \tag{56}$$

and

$$\nabla\phi \sim \mathcal{N}(\overline{\nabla\phi}, \mathbf{C}_{\nabla\phi}), \tag{57}$$

$$\nabla P \sim \mathcal{N}(\overline{\nabla P}, \mathbf{C}_{\nabla P}). \tag{58}$$

We can now simulate the uncertainties associated with determined phase and amplitude errors. For the following figures, the same two-dimensional intensity probe from Sec. III A is used, and we assume typical calibration errors of $\sigma_P = 0.05$ dB and $\sigma_\phi = 0.05°$. This means that the input pressures are 95% accurate within $\pm 0.1$ dB and $\pm 0.1°$. Frequency independent calibration errors are used for this analysis, though it should be noted that in practice phase mismatch is likely to be worse at low frequencies.

Using these sigma values, a random set of normally distributed pressure amplitudes, $P$, and phase values, $\phi$, are generated. The FD and PAGE methods are then applied to the generated values to estimate the intensity. If we assume the resulting PAGE and FD estimates are multivariate normal distributions, we can estimate the covariance matrix associated with the scattered intensities.[38] This covariance matrix, along with the mean of the resulting intensities, is used to find a 95% ellipse to fit the data. Using more points has negligible effect on the resulting error ellipses, so it is determined that 10 000 intensity estimates is a sufficient sample size. The resulting 95% error ellipses can be seen in Fig. 7. As we can see in Fig. 7, measurement uncertainties of the PAGE and FD methods are nearly equivalent at low frequencies. At higher frequencies, the frequency-dependent bias of the FD method can be seen as the error ellipse is no longer centered around the correct value, but instead the intensity is underestimated.

One insight gained from Fig. 7 is how each method responds to calibration. The magnitude of the uncertainties found through the PAGE method is correlated directly with magnitude calibration errors. For example, increasing $\sigma_P$ results in larger magnitude uncertainties, but has no effect on the angle uncertainties. The uncertainty ellipses from the FD method, on the other hand, do not seem to have as direct of a correlation; increasing $\sigma_P$ affects both the phase and magnitude errors.

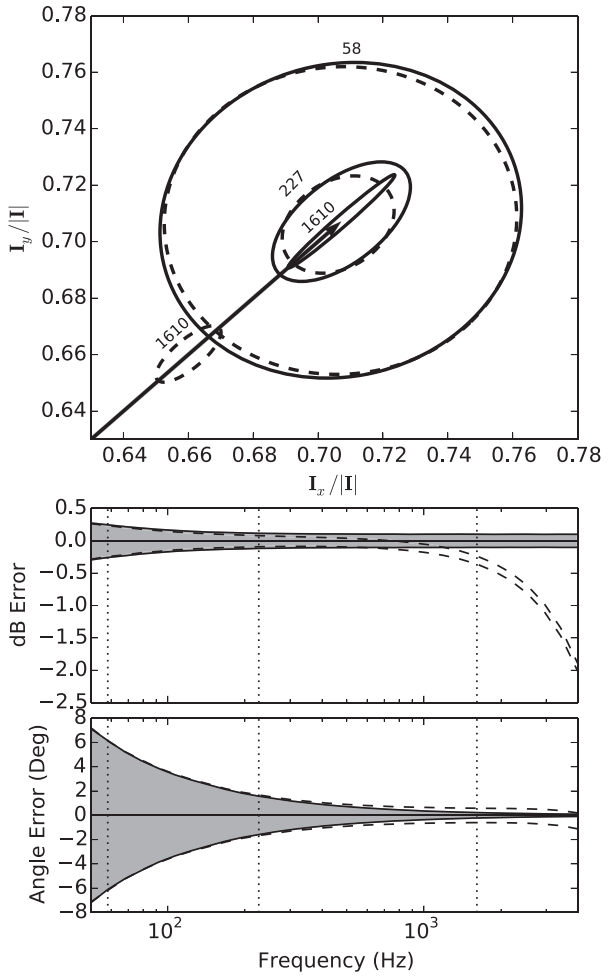


FIG. 7. Uncertainty in magnitude and direction of the intensity found from the 95% confidence ellipses for both the FD (dashed lines, no fill) and PAGE (solid lines, gray fill) methods. Uncertainties are calculated using the two-dimensional probe described in Eq. (A1), and using calibrations errors of $\sigma_P = 0.05$ dB and $\sigma_\phi = 0.05°$. The plot on the top shows three sample error ellipses at frequencies marked by dotted vertical lines on the bottom two plots. The vector in the top plot represents the analytic intensity.

## V. SUMMARY AND CONCLUSIONS

We have presented a least-squares formulation of the gradient estimation technique for arbitrary probe geometries. This method has been applied to the FD method for estimating the acoustic intensity. We also developed a new technique that we have termed the PAGE method by combining finite-difference estimates for the phase and amplitude gradients with the analytical work of Mann and Tichy.[30–32] This method estimates $\nabla\phi$ and $\nabla P$ separately and uses the result to estimate the acoustic intensity. The estimated phase gradient, $\widehat{\nabla\phi}$, is obtained from the pairwise transfer functions of the microphones in the probe. The amplitude gradient, $\widehat{\nabla P}$, is estimated using the resulting pairwise differences of the pressure amplitudes measured at the microphones in the probe. One advantage of the PAGE method is that the estimated phase gradient can be unwrapped in certain cases, which allows for accurate intensity estimates past the spatial Nyquist limit. Special consideration was given when using ensemble averaging with the PAGE method.

The FD and PAGE methods have been compared for three cases: a one-dimensional probe in a plane-wave field, a

two-dimensional probe rotated in a plane-wave field, and the two-dimensional probe in the field produced by three ideal point sources. These cases have been chosen to illustrate the advantages of the PAGE method for estimating the acoustic intensity of plane-wave fields and to show that the advantages persist in more complex systems. It has been shown that for all these cases, the PAGE method estimates exhibit less error than the FD method estimates. The PAGE method produces estimates of the active acoustic intensity with negligible error for plane-wave fields with frequencies below the spatial Nyquist frequency. Furthermore, in the case of the three-source system presented in Fig. 4, the PAGE method has less overall error than the FD method.

Finally, a brief error analysis of the FD and PAGE methods has been presented. It was shown that calibration errors have equal effects on both methods at low frequencies. However, the FD method produces significantly biased results at higher frequencies while the PAGE method has no bias. Furthermore, the robustness of the PAGE method at frequencies above the spatial Nyquist allows for the microphones to be spaced farther apart, which in turn helps to improve the low-frequency estimates.

The PAGE method developed here provides significant advantages over the standard FD method for estimating acoustic intensity. Because the PAGE method uses the same hardware as the FD method, the PAGE method can be used with any existing finite-difference p-p intensity probe. It does not suffer from the same frequency-dependent bias and appears to be more accurate in general.

## APPENDIX: DERIVATION OF FD AND PAGE EQUATIONS FOR TWO-DIMENSIONAL PROBE

The derivations of Eqs. (35)–(37) are demonstrated in this section. Given the probe configuration presented in Eq. (34), the matrix, $\mathbf{X}$, is

$$\mathbf{X} = \begin{bmatrix} (\mathbf{r}_2 - \mathbf{r}_1)^T \\ (\mathbf{r}_3 - \mathbf{r}_1)^T \\ (\mathbf{r}_4 - \mathbf{r}_1)^T \\ (\mathbf{r}_3 - \mathbf{r}_2)^T \\ (\mathbf{r}_4 - \mathbf{r}_2)^T \\ (\mathbf{r}_4 - \mathbf{r}_3)^T \end{bmatrix} = \frac{a}{2} \begin{bmatrix} 0 & 2 \\ \sqrt{3} & -1 \\ -\sqrt{3} & -1 \\ \sqrt{3} & -3 \\ -\sqrt{3} & -3 \\ -2\sqrt{3} & 0 \end{bmatrix}. \tag{A1}$$

The pressure gradient as estimated by the FD method is

$$\widehat{\nabla p} = \frac{1}{3a} \begin{bmatrix} \sqrt{3}(p_3 - p_4) \\ 2p_2 - p_3 - p_4 \end{bmatrix}. \tag{A2}$$

Since $p_1$ is at the center of the probe, $p_0$ is equal to $p_1$, and the estimated complex intensity is given by Eq. (7)

$$\begin{aligned} \widehat{\mathbf{I}}_c^{\mathrm{FD}} &= p\mathbf{u}^* \\ &= p_1 \left( \frac{j}{\rho_0 \omega} \widehat{\nabla p} \right)^* \\ &= \frac{-j}{3\rho_0 \omega a} \begin{bmatrix} \sqrt{3}(p_1 p_3^* - p_1 p_4^*) \\ 2p_1 p_2^* - p_1 p_3^* - p_1 p_4^* \end{bmatrix}, \end{aligned} \tag{A3}$$

or in terms of the one-sided cross-spectrum, $G_{ij} = 2p_i^* p_j$

$$\widehat{\mathbf{I}}_c^{\mathrm{FD}} = \frac{-j}{6\rho_0 \omega a} \begin{bmatrix} \sqrt{3}(G_{31} - G_{41}) \\ 2G_{21} - G_{31} - G_{41} \end{bmatrix}. \tag{A4}$$

In the PAGE method, the pairwise pressure differences used in the FD method are replaced by the argument of pairwise transfer functions. As was shown previously, this is equivalent to the pairwise phase differences. The estimated phase gradient is

$$\widehat{\nabla \phi} = -\frac{1}{3a} \begin{bmatrix} \sqrt{3}\arg\{H_{34}\} \\ \arg\{H_{23}\} + \arg\{H_{24}\} \end{bmatrix}. \tag{A5}$$

The estimated pressure amplitude gradient is

$$\widehat{\nabla P} = \frac{1}{3a} \begin{bmatrix} \sqrt{3}(P_3 - P_4) \\ 2P_2 - P_3 - P_4 \end{bmatrix}. \tag{A6}$$

The pressure amplitude at the probe center is $P_0 = P_1 = |p_1|$. The active and reactive components of acoustic intensity are then estimated by the PAGE method as

$$\widehat{\mathbf{I}}_a^{\mathrm{PAGE}} = -\frac{P_1^2}{6a\omega\rho_0} \begin{bmatrix} \sqrt{3}\arg\{H_{34}\} \\ \arg\{H_{23}\} + \arg\{H_{24}\} \end{bmatrix}, \tag{A7}$$

$$\widehat{\mathbf{I}}_r^{\mathrm{PAGE}} = -\frac{P_1}{6a\omega\rho_0} \begin{bmatrix} \sqrt{3}(P_3 - P_4) \\ 2P_2 - P_3 - P_4 \end{bmatrix}. \tag{A8}$$


[1]IEC 1043:1993, "Electroacoustics—Instruments for the measurement of sound intensity—Measurement with pairs of pressure sensing microphones" (International Electrotechnical Commission, Geneva, Switzerland, 1993).
[2]ANSI/ASA S1.9-1996, *Instruments for the Measurement of Sound Intensity* (Acoustical Society of America, Melville, NY, 1996).
[3]ISO 11205:2003, Acoustics—Noise emitted by machinery and equipment—Engineering method for the determination of emission sound pressure levels *in situ* at the work station and at other specified positions using sound intensity (International Organization for Standardization, Geneva, Switzerland, 2003).
[4]ISO 15186-1:2000, Acoustics—Measurement of sound insulation in buildings and of building elements using sound intensity—Part 1: Laboratory measurements (International Organization for Standardization, Geneva, Switzerland, 2000).
[5]ISO 15186-1:2003, Acoustics—Measurement of sound insulation in buildings and of building elements using sound intensity—Part 1: Field measurements (International Organization for Standardization, Geneva, Switzerland, 2003).
[6]ISO 9614-1:1993, Acoustics—Determination of sound power levels of noise sources using sound intensity—Part 1: Measurement at discrete points (International Organization for Standardization, Geneva, Switzerland, 1993).
[7]ISO 9614-2:1996, Acoustics—Determination of sound power levels of noise sources using sound intensity—Part 2: Measurement by scanning (International Organization for Standardization, Geneva, Switzerland, 1996).
[8]ISO 9614-3:2002, Acoustics—Determination of sound power levels of noise sources using sound intensity—Part 3: Precision method for measurement by scanning (International Organization for Standardization, Geneva, Switzerland, 2002).
[9]F. Fahy, *Sound Intensity* (Spon, London, 2002), pp. 1–295.
[10]F. Jacobsen, "Sound intensity," in *Springer Handbook of Acoustics*, edited by T. D. Rossing (Springer, New York, 2007), pp. 961–1017.
[11]F. Jacobsen, "Sound intensity measurements," in *Handbook of Noise and Vibration Control*, edited by M. J. Crocker (Wiley, Hoboken, NJ, 2007), pp. 534–548.

[12]M. J. Crocker, "Measurement of sound intensity," in *Handbook of Acoustical Measurements and Noise Control*, edited by C. M. Harris (McGraw-Hill, New York, 1991), pp. 14.1–14.17.
[13]U. S. Shirahatti and M. J. Crocker, "Two-microphone finite difference approximation errors in the interference fields of point dipole sources," J. Acoust. Soc. Am. **92**, 258–267 (1992).
[14]R. Raangs, W. F. Druyvesteyn, and H. E. De Bree, "A low-cost intensity probe," J. Audio Eng. Soc. **51**, 344–357 (2003).
[15]J. H. Giraud, K. L. Gee, and J. E. Ellsworth, "Acoustic temperature measurement in a rocket noise field," J. Acoust. Soc. Am. **127**, EL179–EL184 (2010).
[16]K. L. Gee, J. H. Giraud, J. D. Blotter, and S. D. Sommerfeldt, "Energy-based acoustical measurements of rocket noise," AIAA Paper 3165-2009.
[17]K. L. Gee, J. H. Giraud, J. D. Blotter, and S. D. Sommerfeldt, "Near-field acoustic intensity measurements of a small solid rocket motor," J. Acoust. Soc. Am. **128**, EL69–EL74 (2010).
[18]T. A. Stout, K. L. Gee, T. B. Neilsen, A. T. Wall, D. W. Krueger, and M. M. James, "Preliminary analysis of acoustic intensity in a military jet noise field," Proc. Mtgs. Acoust. **19**, 040074 (2013).
[19]J. H. Giraud, K. L. Gee, S. D. Sommerfeldt, T. Taylor, and J. D. Blotter, "Low-frequency calibration of a multidimensional acoustic intensity probe for application to rocket noise," Proc. Mtgs. Acoust. **14**, 040006 (2013).
[20]F. Jacobsen and H.-E. de Bree, "A comparison of two different sound intensity measurement principles," J. Acoust. Soc. Am. **118**, 1510–1517 (2005).
[21]F. Jacobsen, V. Cutanda, and P. M. Juhl, "A numerical and experimental investigation of the performance of sound intensity probes at high frequencies," J. Acoust. Soc. Am. **103**, 953–961 (1998).
[22]G. W. Elko, "Frequency domain estimation of the complex acoustic intensity and acoustic energy density," Ph.D. thesis, The Pennsylvania State University, 1984.
[23]J. W. Parkins, S. D. Sommerfeldt, and J. Tichy, "Error analysis of a practical energy density sensor," J. Acoust. Soc. Am. **108**, 211–222 (2000).
[24]R. Hickling and A. W. Brown, "Determining the direction to a sound source in air using vector sound-intensity probes," J. Acoust. Soc. Am. **129**, 219–224 (2011).
[25]G. Rasmussen, "Measurement of vector fields," in *Proceedings of the 2nd International Congress on Acoustic Intensity* (1985), pp. 53–58.
[26]B. S. Cazzolato and C. H. Hansen, "Errors arising from three-dimensional energy density sensing in one-dimensional sound fields," J. Sound Vib. **236**, 375–400 (2000).
[27]B. S. Cazzolato and C. H. Hansen, "Errors in the measurement of acoustic energy density in one-dimensional sound fields," J. Sound Vib. **236**, 801–831 (2000).
[28]C. P. Wiederhold, "Analytical comparison of multimicrophone probes in measuring acoustic intensity," Master's thesis, Brigham Young University, Provo, UT, 2011.
[29]C. P. Wiederhold, K. L. Gee, J. D. Blotter, S. D. Sommerfeldt, and J. H. Giraud, "Comparison of multimicrophone probe design and processing methods in measuring acoustic intensity," J. Acoust. Soc. Am. **135**, 2797–2807 (2014).
[30]J. A. Mann III, J. Tichy, and A. J. Romano, "Instantaneous and time-averaged energy transfer in acoustic fields," J. Acoust. Soc. Am. **82**, 17–30 (1987).
[31]J. A. Mann III and J. Tichy, "Acoustic intensity analysis: Distinguishing energy propagation and wave-front propagation," J. Acoust. Soc. Am. **90**, 20–25 (1991).
[32]J. A. Mann III and J. Tichy, "Near-field identification of vibration sources, resonant cavities, and diffraction using acoustic intensity measurements," J. Acoust. Soc. Am. **90**, 720–729 (1991).
[33]J.-C. Pascal and J.-F. Li, "A systematic method to obtain 3D finite-difference formulations for acoustic intensity and other energy quantities," J. Sound Vib. **310**, 1093–1111 (2008).
[34]C. P. Wiederhold, K. L. Gee, J. D. Blotter, and S. D. Sommerfeldt, "Comparison of methods for processing acoustic intensity from orthogonal multimicrophone probes," J. Acoust. Soc. Am. **131**, 2841–2852 (2012).
[35]K. H. Miah and E. L. Hixon, "Design and performance evaluation of a broadband three dimensional acoustic intensity measuring system," J. Acoust. Soc. Am. **127**, 2338–2346 (2010).
[36]H. Suzuki, S. Oguro, M. Anzai, and T. Ono, "Performance evaluation of a three dimensional intensity probe," J. Acoust. Soc. Jpn. (E) **16**, 233–238 (1995).
[37]C. A. Szuberla and J. V. Olson, "Uncertainties associated with parameter estimation in atmospheric infrasound arrays," J. Acoust. Soc. Am. **115**, 253–258 (2003).
[38]S. T. Smith, "Covariance, subspace, and intrinsic Cramér-Rao bounds," IEEE Trans. Signal Process. **53**, 1610–1630 (2005).